IR-Based Analysis of Flame Spread in Open and Ceilinged Room Corner Fire Experiments

Belt, A.[1]*, De Lannoye, K.[1], Fehr, M.[2], Arnold, L.[1,2]

[1]*Institute for Advanced Simulation, Forschungszentrum Jülich, Germany*
[2]*Computational Civil Engineering, Bergische Universität Wuppertal, Germany*
**Corresponding author email: a.belt@fz-juelich.de*

ABSTRACT

Three different room corner experiments (RCE) with 6 mm thick poly(methyl methacrylate) (PMMA) panels were carried out in this study. The set-up is located under an exhaust hood and is closed to three sides with brick walls so that air is only entrained via one side. To ensure symmetrical flow conditions, the walls of the RCE were rotated by 45° relative to the room walls and the RCE setup was placed in the middle of the room. As an ignition source, a 10 kW sandbed burner was used. Two open 1 m high RCE configurations and one closed, where an inert calcium silicate ceiling was used, are investigated. In one of the open RCE configurations, the burner was turned off after 2 minutes, to investigate flame spread close to the corner not being dominated by the burner. By including a ceiling, the effect of the radiation feedback is investigated. All experiments were repeated at least three times. Among other measurements, two infrared cameras were used to track the flame front. An in-house software was developed for the IR-based flame front analysis, which will be publicly available. The heat release rate and the temperature measurements between the sample material and the insulation, show a very good repeatability. Furthermore, the analysis of both the IR data and the temperatures show symmetrical behavior between both PMMA plates. It is shown that the ceiling has a strong impact on the flame spread pattern and velocity, the velocity is more than doubled compared to the open RCE configuration. Whereas the effect of turning off the burner for the open room corner is minor, only a small delay in heat release rate is observed.

KEYWORDS: Fire Dynamics, Room Corner Experiment, Flame Spread, poly(methyl methacrylate) (PMMA), Infrared Thermography.

Introduction

Fires in room corner configurations, where two panels are positioned orthogonally with or without a ceiling, are common in various scenarios, such as railway vehicles. Due to increased radiation feedback, room corner fires pose a greater hazard than single wall fires [1,2]. In general, corner fires are frequently considered in flame spread scenarios [3–5], because they spread faster than free burning or single wall fires. For example, Zeinali et al. [6] indicate that corner configurations increase the heat release rate (HRR) contribution of each panel by 45-50 %.

Moreover, unlike parallel wall fires, room corner configurations provide ideal scenarios for investigating and analyzing the interactions between a buoyancy-driven flame and pyrolyzing solid fuels [7]. Accurate modeling of such interactions is necessary for the prediction of fire spread in computational fluid dynamic (CFD) fire models [8,9]. The ability of these models to accurately simulate flame spread depends on the availability of reproducible, systematic, and consistent experimental data across various scales[10–12]. The prediction of fire spread is strongly dependent on the pyrolysis model used within the CFD models. In [13] the state of the art for pyrolysis model parametrization, fire spread and fire growth predictions are summarized. It is pointed out, that a better understanding of the limitations of the current pyrolysis model parametrization approaches is needed and that this can only be achieved

Proc. of the Eleventh International Seminar on Fire and Explosion Hazards (ISFEH11), pp. xx-xx
Edited by J. Chao, V. Molkov, P. Sunderland, F. Tamanini and J. Torero
Published by USTC Press
ISBN: xxx-xxx-xx-xxxx-x :: doi: xx.xxxx/xxx-xxx-xx-xxxx-x_0x-0x

by testing the performance of these approaches against high quality full-scale fire data collected in a wide range of scenarios. While also having corresponding small scale data on the materials used in the large scale experiments.

This study is part of an experimental campaign, funded by the German government. In this project different materials, both rail car specific materials and more fundamental materials, e.g. poly(methyl methacrylate) (PMMA), are experimentally investigated in the milligram-, gram-, and intermediate scale as well as in different room corner configurations (kilogram scale). At the milligram-scale, Microscale Combustion Calorimeter (MCC) and Thermogravimetric Analyser (TGA) experiments are conducted. At the gram-scale, tube furnace experiments with an online mass loss measurement [14] and cone calorimeter experiments are performed. Further, investigations at a horizontal flame spread experiment, which is currently under construction, will be carried out. The results of the kilogram-scale experiments, i.e. RCE, are part of this article. The materials used in this study are systematically investigated at all indicated scales.

In this article, the results of three different configurations of room corner experiments are presented. The baseline configuration consists of two cast black PMMA panels (1 m by 0.5 m, thickness 6 mm), ignited at the bottom by a 10 kW burner. To ensure repeatability, at least three repetitions were performed for each configuration. The HRR of the burner was intentionally kept low compared to other studies, such as that by Dushyant et al. [8], to minimize the influence of the burner on the fire growth.

The presented work focuses on the analysis of the lateral flame spread and the corresponding HRR. To determine the spread, two infrared (IR) cameras and several optical cameras were used and a new software tool was developed. The tool works for both optical and IR data and is publicly available on GitHub [15]. The experiment is conducted beneath an exhaust hood, enabling HRR measurements via the oxygen consumption method integrated into the exhaust system, similar to the single burning item (SBI) test. Additionally, the experimental data will be publicly available.

Experiment set-up

The setup of the experiment is based on ISO 9705-1 [3], two exemplary pictures are shown in figure 1. The base of the experiment is a metal corner structure. Two plates of insulation material (calcium silicate (CaSi), promatect LS, nominal thickness 50 mm) are placed against the upside wall of the corner construction. An additional insulation plate was placed at the bottom of the metal support to protect it from falling sample material and heat.

Two samples were mounted to the insulation in the corner. Black cast PMMA ordered in June 2023 from Evonik Germany (product code 9H01), was used for the experiments. Plates with a width of 50 cm, height of 100 cm and 6 mm thickness were used. The samples were mounted flush with the top of the insulation. An additional piece of insulation is added to cover the top edge of the sample, as previous experiments have shown flame spread over this 6 mm edge independent of the flame spread on the plate, when it is not covered.

Between 20 and 25 screws per plate were used to mount the samples. The configuration of the screws is meant to minimize and delay the folding, bending, and falling of the PMMA pieces during the experiment. In order to reuse insulation material between experiments, three different lengths of screws were used. Furthermore, three different screw patterns were used, the screws were moved by maximum 2 cm compared to the previous patterns. There was no observable influence of the slight difference in screw location on the results of the experiments.

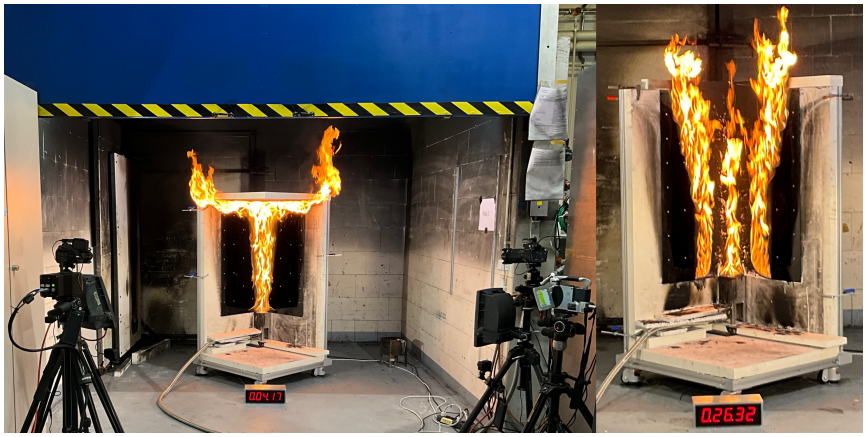

Figure 1. Experiment set-up, left: with ceiling, right: without ceiling.

Samples are ignited using a 100 mm × 100 mm sand-burner, adapted from the ISO 9705-1 standard but with a smaller side. A mass flow of 0.2157 g/s of natural gas is supplied to the burner, resulting in a 10 kW burner. The samples were allowed to burn until spontaneous extinction, at which point all PMMA was burned away.

The set-up is located under a calorimetric hood, allowing for HRR measurements, CO, CO_2 and O_2 measurements for all experiments. The front side of the hood is open (height opening: 1.97 m), the set-up is directed towards the opening at an 45° angle to achieve a mirror-symmetric geometry of the whole experiment. A grid of thermocouples is installed between the backside of the PMMA plates and the insulation material. Two IR cameras: a VarioCAM® HD 876 with a resolution of (1024×768) px and a VarioCAM® HDx head HT with a resolution of (640×480) px were used during the experiments. Each camera was directed to one PMMA plate and recorded images with a frequency of 1 Hz. Optical cameras (Canon 80D) were used to record the experiments for possible flame shape and flame spread analysis. The results from the visual cameras will not be discussed in this contribution. Furthermore, several Sony action cameras were used to document and monitor the experiments.

Three different configurations were tested. The base configuration being two PMMA panels ignited by the burner, which remains on for the full duration of the experiment (V01). In the second series of experiments the burner was turned off after two minutes, at this point the PMMA panels have ignited and self-sustained burning and flame spread is observed (V02). In the third series the burner remains on for the entire experiment but an inert ceiling is placed on top of the corner configuration (V03). The same insulation material is used for the ceiling and a thermocouple grid has been added to measure temperature at the ceiling. Table 1 gives an overview of the different configurations and the dates when the experiments were performed. The experiments have been performed in randomized order, to insure reproducibility over several days. Every experiment configuration was at least run in triplicate. The IR data was captured for at least two repetitions.

Experimental observations

The start of the experiments corresponds to the ignition of the burner. For the base case (V01) without ceiling, the burner remained on for the entire experiment. After 3 to 4 minutes, the flame has reached

Table 1. Overview of experiments

Run	Ceiling	Burner	Configuration	Screws	Date
R1	no	on	V01	A	4 June 24
R2	no	on	V01	A	4 June 24
R3	yes	on	V03	A	4 June 24
R4	no	on	V01	B	5 June 24
R5	no	on	V01	B	5 June 24
R6	yes	on	V03	B	5 June 24
R7	no	off after 2 min	V02	B	6 June 24
R8	no	off after 2 min	V02	B	6 June 24
R9	yes	on	V03	B	6 June 24
R10	no	off after 2 min	V02	C	7 June 24

the top of the sample. From this point on, the flames start spreading horizontally over the surface of both plates. Around 12 minutes into the experiment, some smaller pieces of PMMA (roughly 10 cm by 5 cm) fell down. No attempt was made to extinguish these pieces. Compared to the sample burning area at that moment they are rather small, therefore their contribution to the HRR will be negligible. Near the flame edge, sample deformation (swelling perpendicular to the plate) could be observed. Around 14 minutes into the experiment, the flame spread takes a more pronounced V-shape, the flames are spreading faster at the top of the sample than at the bottom. Around 15 minutes, the material in the middle corner has burned away, resulting in separate flames spreading on each plate. Around 35 minutes, the flame front has reached the top outer corners of the plates. A few minutes later the top edges start deforming, collapse over itself and eventually fall off. Several screws were installed closed to the edge of the sample, to postpone this effect as long as possible. After 1 hour, the sample is completely burned out.

In the V02 experiments, the burner was turned off after 2 minutes. At this point, a small flame with a height of around 70 cm to 80 cm is present in the middle of the sample. At around 4 minutes, this flame has spread to the top, the bottom part of the plate right above the burner has not yet fully ignited. At around 5 minutes, the flames also start spreading vertically. Just as in the V01 case, it is observed that some piece detached from the wall and fall down where they continue burning. This happens slightly later (around 13 minutes and a half) than in the case where the burner remains on the entire time. The rest of the experiment is similar to the description given for V01, with full flame out also being after approximately 1 hour.

The experiments with a ceiling are shorter and more violent. The flame reaches the ceiling quickly – less than 2 minutes after the start of the experiment. At this point, the flame starts spreading in a thin layer right below the ceiling. Resulting in a T-shaped flame. After 3 minutes into the experiment, the full 50 cm width of both panels are ignited at the top. From this point on, the dominant flame spread is downward. Around five and a half minutes, some pieces detach off the wall and continue burning at the bottom of the set-up. More detachment is observed for these experiments than for V01 and V02. Around 14 minutes, the downward flame spread has reached the middle of the plates. The spread has become slower, probably due to the radiation and the confinement of the flame by the ceiling becoming less dominant. The flame continues to spread, but downward flame spread is no longer dominant and the vertical (side wise) spread and downward spread are at similar rates. At this point, some smaller pieces falling off the wall might occasionally ignite parts of the PMMA plate that were not yet burning. At 19 minutes, the flame spread has reached the edge of the sample. After about 40

minutes, the sample is completely burned out. In all three configurations, flame spread on both panels appear to be symmetrically.

Flame front detection

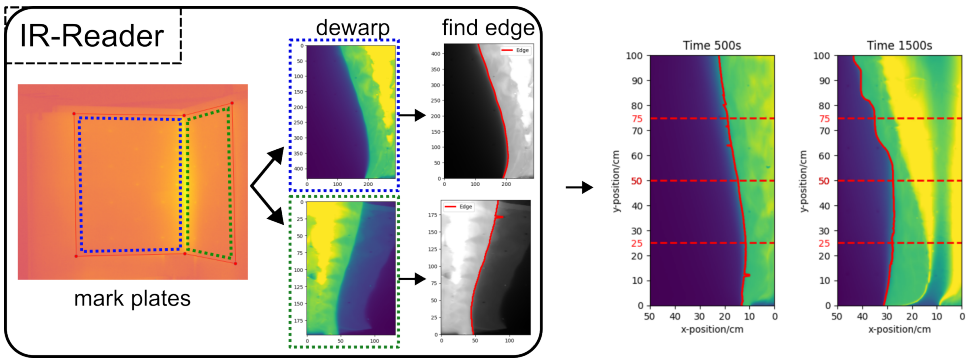

Figure 2. Data-processing from the raw camera file (IBR) to CSV files to extract and analyze flame edge data. The right part indicates the locations (y = 25 cm, 50 cm and 75 cm) of the flame spread analysis presented in this article.

The IR cameras were used to track the flame front. Both cameras store a fixed number of frames per file in a manufacturer specific proprietary file format (IBR). To make the data publicly accessible and ensure broader compatibility, these files were converted into human-readable comma separated value (CSV) files using the IRBIS® 3 Plus software from InfraTec GmbH. Each native IRB file, containing 1200 frames, results in 1200 corresponding CSV files.

Subsequently, these CSV files were processed using the Python based FlameTrack package [15], developed specifically by the authors for this study. This package supports lazy loading of individual frames and provides tools for image manipulation, such as brightness adjustment and setting lower and upper thresholds. In a first step, the user identifies the corners of the PMMA plate in a clockwise sequence, enabling the software to automatically dewarp both visible PMMA-plates in each frame (blue and green dashed fields in right part of figure 2). The dewarped plate images (left and right plates separately) are stored in a H5P file, an open data format chosen for its efficient lazy loading capability.

To find the flame edge in the dewarped images, a band-pass filter is applied to reduce noise and highlight relevant regions by restricting pixel values, which correspond to temperatures in infrared images, to a defined range of 100 °C to 380 °C. The maximum possible value for these pixel-based temperatures is 550 °C. This step ensures that subsequent analysis focuses solely on significant variations in the data. After filtering, the pixel intensities are scaled to a range of 0 to 255 using OpenCV's normalization function, facilitating binary segmentation.

Binary segmentation is conducted using Otsu's thresholding method, which dynamically calculates an optimal threshold to distinguish foreground regions of interest from the background. To enhance the continuity and connectivity of the segmented regions, morphological dilation is applied to the binary mask. Edge detection is then carried out row by row across the mask. For each row, the algorithm identifies the active region (i.e. the flame front) using the binary mask, extracts the corresponding segment from the band-pass filtered non-normalized frame, and determines the edge point closest to the flame start by locating the last pixel exceeding a set intensity threshold of 280. Analyzing

optical data is solely different in that grayscale images are considered instead of temperature data, no bandpass filter is applied, and different threshold values are used (125 instead of 180).

For time-series datasets, background subtraction is used to enhance dynamic features by subtracting the previous frame from the current one, thereby reducing static noise. If edge detection is required on the left side of the frame, the data is flipped horizontally prior to processing, allowing the same detection algorithm to be employed.

Upon completion of the edge detection process, the flame spread along a user-defined height is visualized, facilitating verification of the flame edge extraction accuracy.

During the conversion of the IBR data to CSV files, errors occur at the transitions between files. At these points, the values are removed and replaced with linearly interpolated values, taking into account the neighboring values. Following this, a 5 point moving average, corresponding to a time interval of 5 s, is used to smooth the data, ensuring more consistent flame position tracking. By testing different window sizes, a minimum size of 5 points was chosen to remove noise without removing import features.

The Python package was validated using a different experiment: the standardized lateral flame spread experiment [16]. Black cast PMMA (9H01 by Evonik) plates, 6 mm by 80 cm by 15.5 cm, were ignited by a radiative burner and allowed to spread horizontally until full burn out. During the experiment, recordings were made with both an optical camera (Canon D80) and the aforementioned IR camera (VarioCAM® HD 876). Both cameras were positioned at close to identical locations and captured almost identical frames. Images from both cameras were processed using the Python package. The results are presented in figure 3, demonstrating that the recorded flame spread is nearly identical. Furthermore, the IR recordings produce significantly smoother results, which makes the extensive smoothing necessary in optical camera data unnecessary.

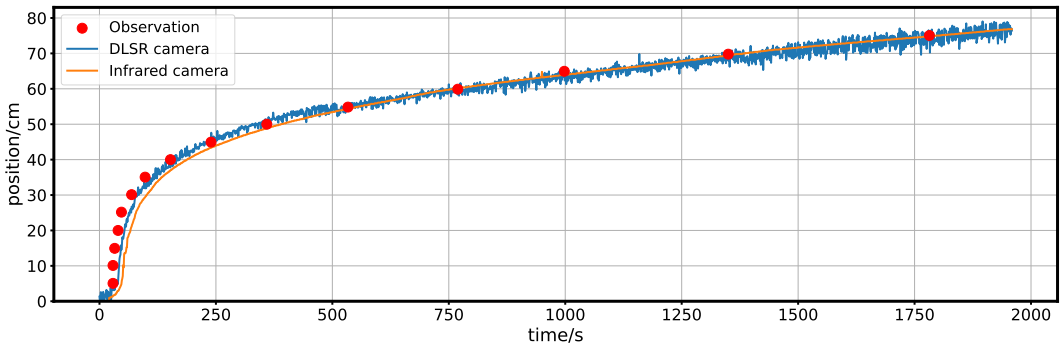

Figure 3. Comparison between the flame front position based on optical data, IR data and data collected by an observer tracking its progress relative to predefined markers during a lateral flame spread experiment.

Results

Figure 4 shows the average HRR curve for each of the configurations. The uncertainty included in the figure is determined by the standard deviation between different repetition experiments, a one sigma interval is shown as uncertainty band. As can be seen from the figure, the HRR is very reproducible between different repetition experiments, maximal deviations are within the range of 6.61 %

to 16.67 %. Note that the experiments were conducted on different days and in mixed order. Thus, the repeatability of the HRR, and eventually the whole experiment, is ensured.

For V03, the peak HRR is 1.8 times higher than for V02. This is due to the confinement and radiation feedback from the ceiling. While the slope of the HRR is very similar for V01 and V02, it is three times as high for V03 compared to V01, which is due to the radiation feedback of the ceiling. Further, subtracting the burner power from V01, besides the slower initial spread, one can see the similarity between V01 and V02. In order to compare the total HRR from all experiments, 10 kW (burner power) is subtracted from V01 and V03. The average total HRR is (159.92 ± 5.04) MJ, indicating that the experiments yield plausible and reproducible (variation of 3.15 %) results with respect to the HRR.

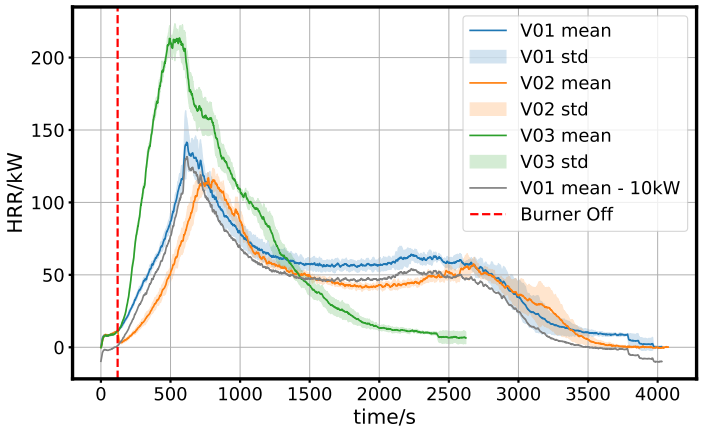

Figure 4. Mean and standard deviation (std) of the HRR for the three different configurations. Additionally, for V01, the mean without the burner contribution (10 kW) is shown.

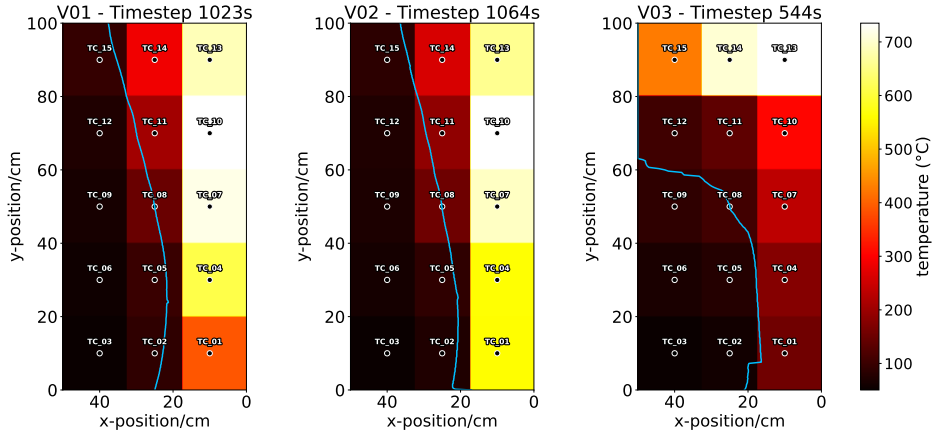

Figure 5. Thermocouple positions and readings at the left PMMA panel, where the position indicates the distance to the center line of the experiment. The blue line shows the position of the flame front. The time steps were chosen to match the time, when the flame front reaches TC_08.

Figure 5 shows the grid of thermocouples located between the left PMMA and the CaSi plate. A total of 15 (5 rows by 3 columns) thermocouples were used for each PMMA plate. The distance between the outer thermocouples, the horizontal and vertical edges of the PMMA plate is 10 cm. The horizontal distance between the thermocouples is 15 cm and the vertical one is 20 cm. The subfigures show the temperature fields and the position of the flame front at a selected time (time at which the flame front reached TC_08). Each measured temperature was assumed for the entire cell from the grid indicated above. The highest temperatures are reached behind the flame front, as more PMMA has burned away resulting in a thinner barrier between the flame and the thermocouple. A detailed analysis of the position of the flame front and the temperature measurements is described below.

Figure 6 shows the horizontal position of the flame front on the left PMMA plate determined by the right IR camera. The flame front location for the three RCE configurations and its standard deviation at three different heights (25 cm, 50 cm and 75 cm) are shown. As can be seen in figure 6, the position of the flame front for the different experiments is in good agreement with respect to repetitions, taking into account the uncertainty resulting from, for example, falling PMMA pieces or deformations of the sample. For the position data, the horizontal resolution varied with camera positions, ranging from 1.52 mm/px to 2.58 mm/px for the left plate. Since this uncertainty is small compared to the overall range it was excluded from the plots. Therefore, the position of the flame front is also very repeatable and thus is assumed to represent a good validation quantity.

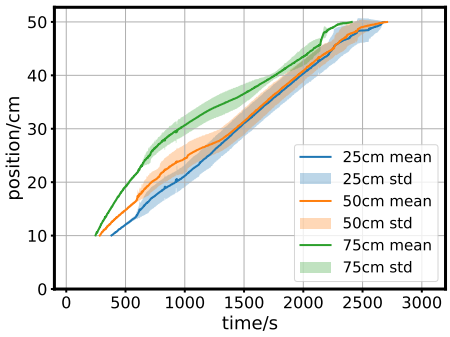

(a) V01

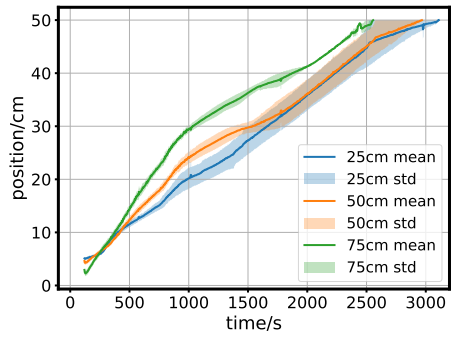

(b) V02

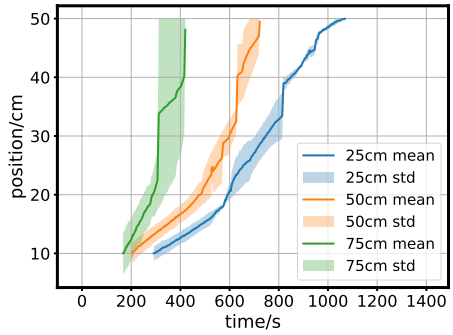

(c) V03

Figure 6. Flame position at three different heights. The time axis range is kept the same for V01 and V02, but is different for V03

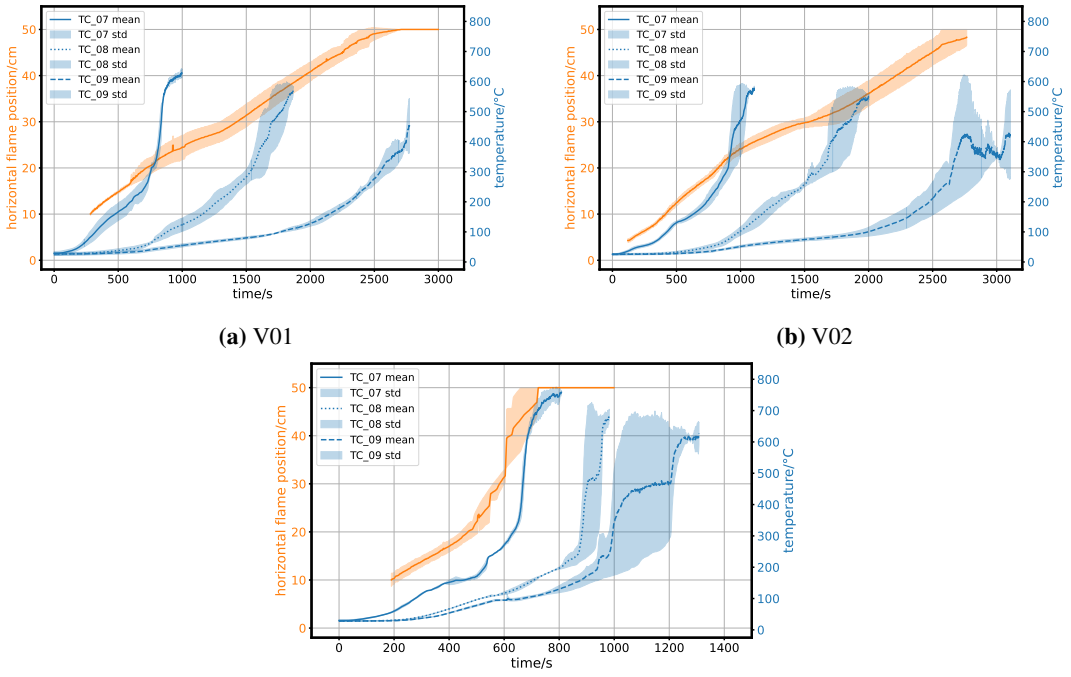

(a) V01

(b) V02

(c) V03

Figure 7. Flame position at 50 cm height and temperature evolution (TC_07, TC_08, TC_09) on the left PMMA slab.

Figure 7 depicts the position of the flame front at a height of 50 cm. The thermocouples (TC_07, TC_08, TC_09) are located at a distance of 10 cm, 25 cm and 40 cm from the center at the same height (y = 50 cm) as the flame position analysis. The temperature data was cut off at its maximum. At this temperature, the PMMA is assumed to be completely pyrolyzed and the thermocouple measures the effects of radiation and convection of the flame, no longer the backside temperature. It is expected that already before the maximum, thermal contact between the thermocouple and the back of the PMMA is lost, due to deformation of the material or no material remaining. For V01 and V02, it can be seen that both the curve of the fire spread and the temperatures are very similar. Only the maximum temperature of TC_07 is significantly higher in V01 than in V02 (50.5 °C). This is due to the burner, which in V01 remains on for the entire experiment, and the position of the thermocouple being very close to the flame area of the burner, it is not related to any difference in sample behavior. For TC_08, T_{max} of V01 and V02 is almost equal which implies, that the effect of the burner on the thermocouple at this position is minor in comparison to the burning PMMA and radiation feedback. It can also be seen that the temperature maxima decrease with increasing distance from the room corner. This shows the influence of less burning material and less radiation feedback from the corner with increasing distance from the room corner. The plot of V03 shows that the temperatures increase much faster compared to V01 and V02, and that there are very large uncertainties for TC_08 and TC_09 in particular after approximately 800 s, which indicates that the thermocouples are no longer measuring the backside temperature of the PMMA.

The field of view of both IR cameras is different. Each of them aims at one of the panels, thus capturing the other panel with a highly inclined angle. Yet, both panels are captured by both cameras but with

different resolutions for each camera. After the dewarp of for example experiment 10, the resolution of the left slab is 494 px × 329 px and the one of the right is 152 px × 100 px. In contrast, dewarping experiments R1 to R3 yields a resulting left image with 454 px × 302 px and 188 px × 125 px for the right image. Nevertheless, the spatial error due to low amount of pixels is with a range of 3.85 mm/px to 5.05 mm/px for the right plate still smaller than the standard deviation and is hence omitted from the plots displaying right plate data.

Figure 8a depicts the propagation of the flame front based on the IR data from the right IR camera for both plates. The artifact seen in the center of the V02 curve, both here and in plot 8b is caused by a tracking error. It can be seen that the flame front behaves very similarly on both slabs, although the one on the right slab appears to be slightly faster for all three configurations, which might be caused by the higher uncertainty due to spatial resolution for the right plate with the right camera.

Figure 8b shows the comparison of the flame spread based on the left and right cameras for the right PMMA plate, at a height of 50 cm. It can be seen that there are only slight differences, probably due to the different camera perspectives.

To further investigate the symmetry of the experiment, temperature data at a height of 50 cm is shown in figure 8c for both panels. The temperature curves were cut off at the temperature maxima, as discussed above. The comparison of the temperature curves also shows the symmetrical behavior of the experiments.

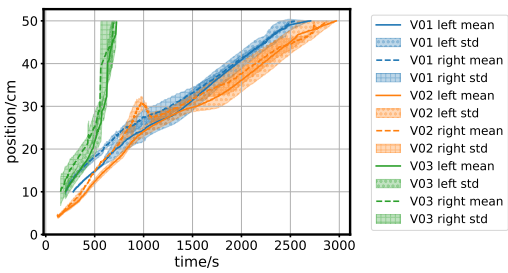

(a) Flame spread on the left and right panel, based on data from the right IR camera.

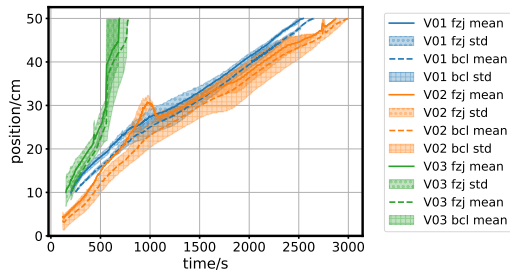

(b) Flame spread on the right panel based on left (FZJ) and right (BCL) IR camera.

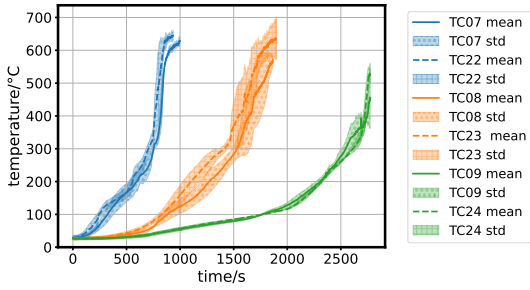

(c) Temperature data (V01) at symmetric thermocouple locations on both panels.

Figure 8. Symmetry analysis based on temperature and IR measurements, all at a height of 50 cm.

Conclusion and Future Work

Three different room corner experiments with at least three repetitions each were carried out. It has been shown that the HRR (especially during fire growth) are very reproducible, despite small uncertainties due to sample deformations and smaller PMMA parts detaching from the wall. Furthermore, the temperature measurements, which were arranged symmetrically on the CaSi plates, show on the one hand that up to a certain time these have good repeatability as well, and on the other hand that the fire propagation takes place symmetrically on the two plates. In addition to conventional single lens reflex cameras, two IR cameras were used for flame tracking. A new open access analysis software was developed to determine the position of the flame front. Experimental data collected at the lateral flame spread test according to [16] was used to validate the method. The software was used both for the IR based analysis and for the analysis of optical images. It was shown that the IR based analysis provides less noisy results and that the photos only lead to usable results with sufficient time averaging. However, this is specific to lateral flame spread. Therefore, only IR data was used to analyze the flame spread of the room corner experiments conducted in this study. These also show, on the one hand, that there is good repeatability and, on the other, that the flame fronts spread symmetrically on the left and right sides of the room corner. The amount of repetitions and the high level of symmetry and reproducibility make this a very valuable dataset for the validation of CFD based flame spread models.

In the near future, the experimental data from MCC and TGA experiments on the same material, will be published as well. Furthermore, experiments with horizontal flame spread will be conducted with the same material and will also be published. Cone calorimeter experiments with this material are still ongoing. Furthermore, a detailed characterization of the burner will be performed to better specify the according boundary conditions.

Data Availability

The accepted version of the manuscript will contain a link to an open access Zenodo data repository, containing the raw and processed data presented here.

Acknowledgements

This work is part of the BESKID project (Design fire simulations in rail vehicles using AI-based data), funded by the German Federal Ministry of Education and Research (BMBF) with the funding number 13N16392. The authors would like to thank Alica Kandler, Minh Tam Würzburger, Kilian Hager, Anna Troff and Manuel Osburg for their support with conducting these experiments. The software for tracking the flame front was validated using experiments funded by the VIB (Verein zur Förderung von Ingenieurmethoden im Brandschutz, English: Association for the Support of Fire Safety Engineering).

REFERENCES

1. Takahashi, W., Tanaka, H., and Ohtake, M. Flame and Plume Behavior in and near a Corner of Walls. *Fire Safety Science - Proceedings of the Fifth International Symposium, Melbourne, Australia*, pages 261–271, 1997. doi: 10.3801/iafss.fss.5-261.
2. Poreh, M. and Garrad, G. Study of Wall and Corner Fire Plumes. *Fire Safety Journal*, pages 81–98, 2000. doi: 10.1016/S0379-7112(99)00040-5.
3. ISO 9705-1. Reaction to fire tests — Room corner test for wall and ceiling lining products — Part 1: Test method for a small room configuration. Standard, International Organization for

Standardization, Geneva, CH, 2016.

4. NFPA 286. Standard Methods of Fire Tests for Evaluating Contribution of Wall and Ceiling Interior Finish to Room Fire Growth Scope. Standard, National Fire Protection Association (NFPA), Quincy, Massachusetts, USA, 2019.
5. EN 13823. Reaction to Fire Tests for Building Products - Building Products Excluding Floorings Exposed to the Thermal Attack by a Single Burning Item. Standard, European Standard, 2014.
6. Zeinali, D., Vandemoortele, E., Verstockt, S., Beji, T., Maragkos, G., and Merci, B. Experimental study of corner wall fires with one or two combustible walls. *Fire Safety Journal*, 121:103265, 2021. ISSN 0379-7112. doi: https://doi.org/10.1016/j.firesaf.2020.103265.
7. Torero, J. L. Scaling-up fire. *Proceedings of the Combustion Institute*, pages 99–124, 2013. doi: 10.1016/j.proci.2012.09.007.
8. Chaudhari, D. M., Fiola, G. J., and Stoliarov, S. Experimental analysis and modeling of Buoyancy-driven flame spread on cast poly(methyl methacrylate) in corner configuration. *Polymer Degradation and Stability*, 183:98–119, 2021.
9. Rogaume, T. Thermal decomposition and pyrolysis of solid fuels: Objectives, challenges and modelling. *Fire Safety Journal*, 106:177–188, 2019. doi: 10.1016/j.firesaf.2019.04.016.
10. McGrattan, K., Bareham, S., and Stroup, D. Cable Heat Release, Ignition, and Spread in Tray Installations During Fire (CHRISTIFIRE) Phase 2: Vertical Shafts and Corridors. Technical report, National Institute of Standards and Technology Engineering Laboratory; Fire Research Division Gaithersburg, Maryland 20899, December 2013.
11. Leventon, I. T., Batiot, B., Bruns, M. C., Hostikka, S., Nakamura, Y., Reszka, P., Rogaume, T., and Stoliarov, S. I. The MaCFP Condensed Phase Working Group: A Structured, Global Effort towards Pyrolysis Model Development. In Morgan C. Bruns, editor, *Obtaining Data for Fire Growth Models*, pages 10–29. ASTM International, 100 Barr Harbor Drive, PO Box C700, West Conshohocken, PA 19428-2959, March 2023. ISBN 978-0-8031-7731-4. doi: 10.1520/STP164220210111.
12. Hehnen, T. and Arnold, L. PMMA pyrolysis simulation – from micro- to real-scale. *Fire Safety Journal*, 141:103926, 2023. ISSN 0379-7112. doi: https://doi.org/10.1016/j.firesaf.2023.103926.
13. Stoliarov, S.I. and Ding, Y. Pyrolysis model parameterization and fire growth prediction: The state of the art. *Fire Safety Journal*, 140:103905, 2023. ISSN 0379-7112. doi: https://doi.org/10.1016/j.firesaf.2023.103905.
14. De Lannoye, K., Belt, A., Reinecke, E.-A., and Arnold, L. The tube furnace with online mass loss measurement as a new bench scale test for pyrolysis. *Fire Technology*, 60:3689–3707, 2024. doi: https://doi.org/10.1007/s10694-024-01590-0.
15. Wurzburger, M.T., Fehr, M., and Belt, A. Firedynamics/flametrack: Initial release, January 2025. URL 10.5281/zenodo.14633209.
16. ASTM International. ASTM E1321-18 standard test method for determining material ignition and flame spread properties, 2018.